NASA Technical Memorandum 88854

Concentrated Mass Effects on the Flutter of a Composite Advanced Turboprop Model

J.K. Ramsey and K.R.V. Kaza
Lewis Research Center
Cleveland, Ohio

October 1986

NASA

CONCENTRATED MASS EFFECTS ON THE FLUTTER OF A COMPOSITE ADVANCED TURBOPROP MODEL

J.K. Ramsey and K.R.V. Kaza
National Aeronautics and Space Administration
Lewis Research Center
Cleveland, Ohio 44135

SUMMARY

The effects on bending-torsion flutter due to the addition of a concentrated mass to an advanced turboprop model blade with rigid hub are studied. Specifically the effects of the magnitude and location of added mass on the natural frequencies, mode shapes, critical interblade phase angle, and flutter Mach number are analytically investigated. The flutter of a propfan model is shown to be sensitive to the change in mass distribution. Static unbalance effects, like those for fixed wings, were shown to occur as the concentrated mass was moved from the leading edge to the trailing edge with the exception of one mass location. Mass balancing is also inferred to be a feasible method for increasing the flutter speed.

INTRODUCTION

It is recognized that the inclusion of geometric nonlinearities and aerodynamic coupling (cascade effects) between the blades should be included in the formulation of aeroelastic models for advanced turboprops (propfans). Furthermore, wind tunnel model tests revealed that flutter speed is very sensitive to the position of strain gauges and associated wires. However, it was not apparent whether a change in mass or its distribution, damping of the associated wires, or a change in the aerodynamics, or a combination of all, that resulted in the change in flutter speed. The effects of concentrated mass and its location on the flutter of a propfan is the subject of the present investigation. This investigation was conducted by utilizing an available analytical model of a wind tunnel research propfan model known as the SR3C-X2. The experimental flutter results for the SR3C-X2 propfan are given in reference 1.

The flutter analysis, with and without concentrated mass, was performed using ASTROP (Aeroelastic STability and Response Of Propfans), a code developed at NASA Lewis (ref. 2). The structural model used in this code is represented by blade geometry and the normal modes and frequencies of the rotating blade including geometric nonlinear effects. The aerodynamic portion of the code is based on three-dimensional, unsteady, linear aerodynamics with a constant pressure panel discretization (refs. 3 to 5).

The effects of center of gravity location with respect to the elastic axis on the flutter speed of fixed wings are investigated in references 6 to 9 as well as others. The elastic axes of fixed wings are usually straight, or nearly so. This local distance between the elastic axis and the center of gravity is known as static unbalance. For fixed wings, the flutter speed generally decreases as the center of gravity is moved aft of the elastic axis towards the trailing edge (t.e.). It is therefore desirable to locate the

center of gravity ahead of the elastic axis towards the l.e. Therefore, static unbalance is a very important factor on flutter of fixed wings.

Turbofan blades are thin and exhibit very little sweep if any, and have a large pretwist. The elastic axis also tends to be straight. Cascade effects are strong. The effects of elastic axis and center of gravity position on flutter of turbofan blades are investigated in references 10 to 13, among others.

Propfan blades have large sweep and twist, and are thin and flexible. These blades are usually of low aspect ratio. The elastic axis of a propfan blade is not straight and may not lie on the blade itself. To the best of the authors' knowledge, the effects of adding a concentrated mass at several blade radius stations near the tip, on the flutter Mach number, flutter frequency and natural modes are not found in the literature. By positioning concentrated mass at various locations from the l.e. to the t.e. at a given blade radius section, it will be possible to determine the qualitative effects of concentrated mass location on flutter speed.

ANALYTICAL MODEL

The SR3C-X2 propfan consists of eight blades. The graphite/epoxy blades have 20 percent of the ply lay-ups at $\pm 22.5°$ with respect to the pitch axis, or the Z axis, whereas the remainder of the ply lay-ups are parallel to the pitch axis. A COSMIC NASTRAN finite element model of the SR3C-X2 propfan (ref. 1) blade is shown in figure 1.

NASTRAN input data already existed at NASA Lewis for the SR3C-X2 blade for an rpm of 6950 with a blade pitch angle of 56.4° at the three quarter radius. For convenience this blade and operating condition were chosen for this analytical study. The finite element model (fig. 1) was developed by W.L. Tanksley and Associates, Inc. under NASA contract. The analytical blade model which is clamped at the root consists of 388 CTRIA2 elements and has a tip radius of 0.31 m. Due to the assumption that the blades are not structurally coupled with each other, only one blade was modelled using NASTRAN. The actual number of blades on the propfan was specified within ASTROP. So when a concentrated mass was added to one blade model, it was in effect added to the other seven blades as well. The concentrated masses were assumed to have no mass moment of inertia about their own axis.

The values chosen for the magnitude of the concentrated mass were 0.1, 0.2, 0.5, and 1.0 percent of the total blade mass. The NASTRAN calculated composite blade mass was 161 grams.

As shown in figure 2, 10 grid points were chosen to position the concentrated mass. At the 100 percent radius: 13 percent chord (g.p. 221), 51 percent chord (g.p. 224), and 88 percent chord (g.p. 227). At the 94 percent radius: 0 percent chord (g.p. 202), 51 percent chord (g.p. 206), 88 percent chord (g.p. 209), and 100 percent chord (g.p. 210). At the 82 percent radius: 0 percent chord (g.p. 175), 51 percent chord (g.p. 179), and 100 percent chord (g.p. 183).

PROCEDURE

COBSTRAN (COmposite Blade STRuctural ANalysis), a preprocessor to NASTRAN developed at NASA Lewis (ref. 14), was used to generate the connectivity and the equivalent anisotropic material property cards for use in NASTRAN, from the composite blade lay-up. The concentrated mass was added to the NASTRAN blade model by use of the CONM2 bulk data card (ref. 15). Using the COSMIC NASTRAN static analysis with differential stiffness, the differential stiffness matrix was obtained. This was followed by an eigen analysis using the total stiffness matrix.

For the NASTRAN analyses the blade is considered to be rotating in a vacuum, and hence only centrifugal loads are acting on the blade. Using the first six eigenvectors the flutter Mach number, flutter frequency and critical interblade phase angle were calculated using ASTROP. The flight Mach number is specified by the user. For each interblade phase angle, ASTROP assumes a flutter frequency and the complex eigenvalue for each mode. The real part of the eigenvalue corresponds to the damping and the imaginary part to the frequency. From these damping and frequency values ASTROP calculates a "matched frequency" and the corresponding damping for the interblade phase angle by iterating on the assumed flutter frequency. This is done for each phase angle. The Mach number is then varied by the user until the damping is near zero. The interblade phase angle that first exhibits a zero damping is the critical interblade phase angle. Linear interpolation is performed by the user to calculate the flutter frequency and flutter Mach number corresponding to zero damping.

RESULTS

A vast number of geometric locations and mass magnitudes could have been chosen for this study. However, to keep this investigation within reason a minimum number of cases were selected which would give a qualitative understanding of concentrated mass effects on flutter. These selected cases are presented in table I. The natural frequencies and mode shapes obtained from NASTRAN represent the natural frequency of the SR3C-X2 blade rotating at 6950 rpm with no aerodynamic loading. The flutter Mach number is based on the speed of sound being 339.85 m/sec, at an atmospheric pressure of 93764 N/m^2 and air density of 1.1366 kg/m^3. For an rpm of 6950, wind tunnel or flight Mach numbers less than 0.46 result in large steady-state angles of attack. Therefore, for flight flutter Mach numbers less than 0.46 the aerodynamic model, which assumes small steady-state angles of attack, is stretched beyond its limits of applicability. However, calculated flutter Mach numbers below 0.46 and their associated interblade phase angles and frequencies are qualitatively meaningful in that they help better define the various trends.

Natural Frequencies

The natural frequencies of the blades with concentrated mass located at the 100, 94, and 88 percent radius stations are tabulated in tables II, III, and IV respectively. Also included in the tables for comparison, are the natural frequencies of the reference blade which has no concentrated mass. The first mode is predominantly flatwise bending, the second mode is predominantly torsional, and the third mode is predominantly second flatwise bending.

Only three modes are presented because the flutter mode, which will be discussed later, is a coupling of the first and second modes and is not affected appreciably by the higher modes.

For the 100 percent radius (table II) it is shown that the natural frequencies for the first and second modes increases as the mass is moved towards the l.e. This is true for all the mass magnitudes. However, the addition of these masses keeps the first and second mode frequencies below that of the reference model. The natural frequency for the third mode is highest when the mass is located at the 51 percent chord. At this point the natural frequency is higher than that of the reference model. This is attributed to centrifugal stiffening effects.

At the 94 percent radius (table III), the first mode frequency increases as the mass is positioned towards the l.e. The highest second and third mode frequencies are shown to occur when the mass is located at the 51 percent chord. The lowest second and third mode frequencies occur when the mass is located at the trailing edge, except for the 1.0 percent mass. Here the second mode natural frequency is higher than that calculated for the same mass at the 88 percent chord.

For the 82 percent radius (table IV), as the mass is moved from the t.e. to the l.e. the first and third mode frequencies increase. The highest second mode frequency occurs when the mass is located at the 51 percent chord. The lowest second mode frequency occurs when the mass is located at the t.e.

Mode Shapes

The first three natural (in vacuum) mode shapes for the SR3C-X2 blade at 6950 rpm are shown in figure 3. The change in the first and second mode shapes of the reference model, when the 0.5 percent mass is moved from the 13 percent chord to the 88 percent chord at the 100 percent radius are shown in figures 4, 5, and 6 respectively. As the mass is moved from the 13 percent chord to the 88 percent chord, it can be seen that the first mode shape changes negligibly, whereas the second mode nodal line shifts closer to the t.e.

Due to the change in trends encountered as a result of adding the 1.0 percent mass at the t.e. of the 94 percent radius station, the first and second mode shapes for the 1.0 percent mass located there are presented in figure 7. The addition of the 1.0 percent mass at the t.e. created a localized flapping motion of the blade tip trailing edge. This flapping motion of the tip was observed using the animation capability of EZPLOT, a graphics package developed at NASA Lewis. It is shown in figure 7 that instead of one nodal line for the second mode, there are two. The additional nodal line runs from the tip of the blade to just above grid point 210. This altered mode shape is a contributing factor to the increase in the flutter Mach number (M_f = 0.60), which will be discussed further in the next section.

Flutter Results

The flutter speed of a propfan blade may be characterized by one of several parameters such as: the wind tunnel Mach number (flight Mach number); rotational speed or equivalent blade Mach number at the blade tip; or blade

helical Mach number which corresponds to the blade relative speed at a reference radius. In this report wind tunnel Mach number at a given rotational speed is chosen to characterize the flutter speed.

The other parameters associated with flutter are the reduced frequency and the interblade phase angle. The reduced frequency is calculated at the three quarter radius and is based on the blade semi chord. The number of possible interblade phase angles are given by the relation:

$$\sigma_r = 360\ r/N \qquad r = 0, 1, 2, \ldots N-1$$

where N is the number of blades. The blade numbering sequence and direction of rotation are shown in figure 8. For the SR3C-X2 there are eight blades and hence the possible interblade phase angles are 0, 45, 90, 135, 180, 225, 270, and 315°, respectively. The phase angles of 45, 90, and 135° correspond to forward traveling waves which are in the direction of rotation. The phase angles of 225, 270, and 315° correspond to backward traveling waves which are in the direction opposite to the rotation. The phase angles of 0 and 180° are standing waves.

100 percent radius. - The variation of the flutter Mach number, flutter frequency, and critical interblade phase angle with mass magnitude and location for the 100 percent radius station are shown in figures 9, 10, and 11, respectively. For comparison the reference configuration (no concentrated mass) is also included. For the reference configuration, the flutter Mach number, flutter frequency and the least stable interblade phase angles are: 0.54, 304 cycles/sec, and 225°, respectively.

It can be seen from figure 9, that for a given concentrated mass at the 100 percent radius station the flutter Mach number decreases as the mass is moved towards the t.e. The flutter Mach number is increased above that of the reference model when the mass is located at the 13 percent chord. When the concentrated mass is located at the 51 percent chord, and the 88 percent chord, the flutter Mach number is decreased below that for the reference model.

The reason for the change in flutter Mach number with respect to concentrated mass position can be explained by idealizing the blade as a typical section with two degrees of freedom. The first mode can be thought of as one of uncoupled bending and the second mode as one of uncoupled first torsion. The elastic axis position for the section lies in front of the leading edge because of the blade sweep. The center of gravity is approximately between 40 and 50 percent chord for the reference configuration. When the mass is added at the leading edge the distance between the elastic axis and center of gravity is reduced. This will cause an increase in the flutter Mach number (ref. 8). When the mass is added at the trailing edge the distance between the elastic axis and the center of gravity is increased. This will decrease the flutter Mach number.

Figure 10 shows that the addition of the concentrated masses at the 13 and 51 percent chord decreased the flutter frequency below that of the reference model. At the 88 percent chord the 0.1 percent mass increased the flutter frequency above that of the reference model, whereas the 0.5 and 1.0 percent mass resulted in a decrease in the flutter frequency.

Figure 11 shows the critical interblade phase angle to be 225° for all the concentrated masses at the 13 and 51 percent chord. At the 88 percent chord the 0.1 percent mass produced a phase angle of 180°, whereas the 0.5 and 1.0 percent masses resulted in a critical interblade phase angle of 135°.

94 percent radius. - The variation of the flutter Mach number, flutter frequency, and critical interblade phase angle with mass magnitude and location are shown in figures 12, 13, and 14. Figure 12 shows that as the mass is increased at the l.e. the flutter Mach number increases. The 0.1 percent mass gives a flutter Mach number slightly above that for the reference model. The 0.5 and 1.0 percent masses resulted in more of an increase in the flutter Mach number above the reference model. At the 51 percent chord, the 0.1 percent mass gives no significant change in the flutter mach number. Here, the 0.5 and 1.0 percent masses result in a slight increase in the flutter Mach number.

When the 1.0 percent mass was located at the t.e., the flutter Mach number was calculated to be above that of the reference model. This result seemed peculiar, in that the flutter Mach number was shown to decrease with the addition of mass at the t.e., for the other radius stations. However, the altered second mode shape (see fig. 7) may be the cause of the increase in the flutter speed. Because of the different trend encountered here, additional data points were chosen to help define this change. It was desired to see the effects of concentrated mass at locations close to the t.e. Therefore a 0.2 percent mass was located at the t.e. for one data point and a 1.0 percent mass was located at the 88 percent chord for another data point. At the 88 percent chord, the addition of the 1.0 percent mass decreased the flutter Mach number to 0.30. This result agreed with the trends at the other radius stations. At the t.e., the 0.1 and 0.2 percent masses also resulted in a decrease in the flutter Mach number from that of the reference model. The 0.5 percent mass resulted in a decrease in the flutter Mach number to $M_f = 0.17$. Again, it should be mentioned that for Mach numbers less than 0.46 the steady-state angle of attack of the blades are large and hence the aerodynamic model which assumes small steady-state angles of attack is stretched beyond its limits of applicability. However, calculated flutter Mach numbers below 0.46 and their associated interblade phase angles and frequencies are considered to be meaningful in that they help define the various trends in a qualitative manner.

Figure 13 shows that the addition of the masses at the 51 percent chord and at the l.e., decreased the flutter frequency below that of the reference model. At the t.e. the addition of the 0.1 and 0.2 percent masses increased the flutter frequency above that of the reference model, whereas the 0.5 and 1.0 percent masses decrease the flutter frequency below that of the reference model. At the 88 percent chord, the 1.0 percent mass also decreased the flutter frequency below that of the reference.

Figure 14 shows the interblade phase angle to be 225° for the masses located at the l.e. and at the 51 percent chord. At the t.e. the 0.1 and 0.2 percent masses produced a critical interblade phase angle of 180°, whereas the 0.5 and 1.0 percent masses resulted in a critical interblade phase angle of 135°. The 1.0 percent mass located at 88 percent chord resulted in a critical interblade phase angle of 180°.

82 percent radius. - Figures 15, 16, and 17, show the flutter Mach number, flutter frequency, and critical interblade phase angle for the various added concentrated masses respectively. Figure 15 shows that increasing the mass at

the t.e. decreases the flutter Mach number, whereas increasing the mass at the l.e. increases the flutter Mach number. At the l.e. and at the 51 percent chord the 0.1 percent mass gave no significant increase in the flutter Mach number, whereas the 0.5 and 1.0 percent masses did result in a higher flutter Mach number. At the 51 percent chord the 1.0 percent mass resulted in the highest flutter Mach number for this radius station. At the t.e., the 1.0 percent mass resulted in a flutter Mach number of 0.25.

Figure 16 shows the flutter frequency to be reduced below the reference model by the addition of the concentrated masses at the 51 percent chord and at the l.e. At the t.e., the 0.1 and 0.5 percent masses resulted in an increase in the flutter frequency, the 0.5 percent mass resulting in the highest value. Here, the 1.0 percent mass decreased the flutter frequency below that of the reference model.

Figure 17 shows the critical interblade phase angle to be 225° for all masses located at the 51 percent chord. At the l.e. the 0.1 and 0.5 percent masses produced a critical interblade phase angle of 225°, whereas the 1.0 percent mass resulted in a critical interblade phase angle of 180°. At the t.e., the 0.5 and 1.0 percent mass produced a critical interblade phase angle of 135°, whereas the 0.1 percent mass resulted in a critical interblade phase angle of 180°.

CONCLUSION

This analytical investigation was undertaken to determine how the natural frequencies, critical interblade phase angle, and flutter Mach number of a propfan would be affected by attaching a concentrated mass of various magnitudes (from 0.1 percent to 1.0 percent of total blade mass) at different radial and chord locations in the tip region of the blades. The conclusions pertain to the SR3C-X2 model propfan for the limited number of different concentrated masses and geometric or grid point locations used. Although the scope of the study is limited, the conclusions are important in that they give some insight into mass effects and lay the ground work for future research in this area. The conclusions from this analytical investigation are given below.

1. The results show that any mass on the order of 0.1 percent of the blade mass or greater, mounted in the tip region of the blade will effect the flight flutter Mach number.

2. The flight flutter Mach number is sensitive to the change in natural mode shapes, which are in turn sensitive to changes in mass distribution.

3. In general the addition of the concentrated masses reduced the first, second, and third mode natural frequencies. However, the third mode natural frequency increased slightly by the addition of mass at the 51 percent chord at the 100 percent radius.

4. The flutter Mach number decreased as the mass was moved from the leading edge towards the trailing edge except when the 1.0 percent mass was located at the t.e. at the 94 percent radius station. Except for this one case, the effects of static unbalance are like those for a typical fixed wing section.

5. It appears that locating a mass near the tip region at the l.e. is beneficial for the delay of flutter.

6. Even though mass balancing was not performed in this investigation, it can be inferred from the results of this study that mass balancing would be a feasible method for the delay of flutter.

REFERENCES

1. Mehmed, O.; and Kaza, K.R.V.: Experimental Classical Flutter Results of a Composite Advanced Turboprop Model. NASA TM-88792, 1986.

2. Kaza, K.R.V.; Mehmed, O.; and Murthy, D.V.: Analytical Flutter Investigation of Composite Advanced Turboprop Model. Submitted for presentation at the AIAA/ASME/ASCE/AHS 28th Structures, Structural Dynamics and Materials Conference, Monterey, CA, Apr.6-8, 1987,.

3. Williams, M.H.; Hwang, C-C: Three Dimensional Aerodynamics and Aeorelastic Response of Advanced Turboprops. AIAA/ASME/ASCE/AHS 27th Structures, Structural Dynamics and Materials Conference, San Antonio, TX, May 19-21, 1986. (AIAA Paper 86-0846-CP).

4. Williams, M.H.: User's Guide to UPROP3S, a Program for the Unsteady Aerodynamic Analysis of Single Rotation Propellers. School of Aeronautics and Astronautics, Purdue University, Jan. 1985.

5. Williams, M.H.: An Unsteady Lifting Surface Theory for Single Rotation Propellers. School of Aeronautics and Astronautics, Purdue University, June 1985.

6. Bisplinghoff, R.L.; Ashley, H.; and Halfman, R.: Aeroelasticity. Addison - Wesley, 1955, p. 544.

7. Runyan, H.L.; and Sewall, J.L.: Experimental Investigation of the Effects of Concentrated Weights on Flutter Characteristics of a Straight Cantilever Wing. NACA TN-1594, 1948.

8. Pines, S.: An Elementary Explanation of the Flutter Mechanism. Dynamics and Aeroelasticity, Proceedings of the National Specialists Meeting on Dynamics and Aeroelasticity, Ft. Worth, TX, Nov. 1958, pp. 52-58.

9. Dowell, E.H.; et al.: A Modern Course in Aeroelasticity, Sitjhoff and Noordhoff International Publishers, 1980, p. 111.

10. Bendickson, O.; and Freidmann, P.: Coupled Bending-Torsion Flutter in Cascades. AIAA J. vol. 18, no. 2, Feb. 1980, pp. 194-201.

11. Kaza, K.R.V.; Kielb, R.E.: Flutter and Response of a Mistuned Cascade in Incompressible Flow. AIAA J. vol. 20, no. 8, Aug. 1982, pp. 1120-1127.

12. Kielb, R.E.; and Kaza, K.R.V.: Aeroelastic Characteristics of a Cascade of Mistuned Blades in Subsonic and Supersonic Flows. Journal of Vibration, Acoustics, Stress and Reliability of Design, vol. 105, no.4, Oct. 1983, pp. 425-433.

13. Kielb, R.E.: Mass Balancing of Hollow Fan Blades. ASME Paper 86-GT-195, June 1986.

14. Chamis, C.C.: Integrated Analysis of Engine Structures. NASA TM-82713, 1981.

15. The NASTRAN User's Manual, NASA SP-222(06), 1983.

TABLE I. - SUMMARY OF CASES STUDIED BY PERCENT MASS OF COMPOSITE BLADE (6950 RPM, BLADE SETTING ANGLE 56.4°, BLADE MASS 161 g)

Percent radius	Percent chord				
	100	88	51	13	0
100		1.0, 0.5, 0.1	1.0, 0.5, 0.1	1.0, 0.5, 0.1	
94	1.0, 0.5, 0.2, 0.1	1.0	1.0, 0.5, 0.1		1.0, 0.5, 0.1
82	1.0, 0.5, 0.1		1.0, 0.5, 0.1		1.0, 0.5, 0.1

TABLE II. - NATURAL FREQUENCIES (CPS) WITH AND WITHOUT ADDED MASS AT 100 PERCENT RADIUS (6950 RPM, BLADE SETTING ANGLE 56.4°)

Percent mass	Percent chord from l.e.	Mode		
		1	2	3
Reference mode[a]	- -	228	407	701
1.0	13	212	406	608
	51	203	390	707
	88	185	336	570
0.5	13	220	407	652
	51	215	398	704
	88	205	361	606
0.1	13	227	407	692
	51	226	405	702
	88	224	396	681

[a]No concentrated mass.

TABLE III. - NATURAL FREQUENCIES (CPS) WITH AND WITHOUT ADDED MASS AT 94 PERCENT RADIUS (6950 RPM, BLADE SETTING ANGLE 56.4°)

Percent mass	Percent chord from l.e.	Mode		
		1	2	3
Reference model[a]	---	228	407	701
1.0	0	222	393	642
	51	214	403	682
	88	194	348	612
	100	189	358	560
0.5	0	225	400	671
	51	221	405	691
	100	200	326	540
0.1	0	228	406	695
	51	227	407	699
	100	223	390	654
0.2	100	218	372	611

[a]No concentrated mass.

TABLE IV. - NATURAL FREQUENCIES (CPS) WITH AND WITHOUT ADDED MASS AT 82 PERCENT RADIUS (6950 RPM, BLADE SETTING ANGLE 56.4°)

Percent mass	Percent chord from l.e.	Mode		
		1	2	3
Reference model[a]	---	228	407	701
1.0	0	227	393	700
	51	225	403	687
	100	201	339	596
0.5	0	228	400	701
	51	226	405	694
	100	215	368	635
0.1	0	228	406	701
	51	228	407	700
	100	226	399	685

[a]No concentrated mass

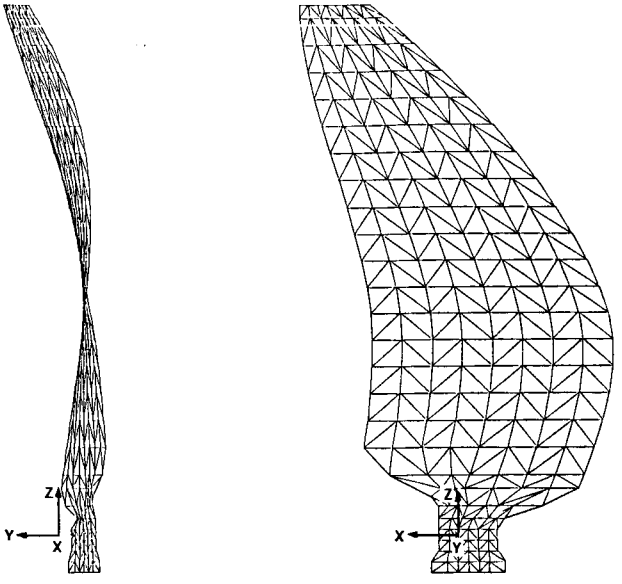

FIGURE 1.- SR3C-X2 FINITE ELEMENT MODEL.

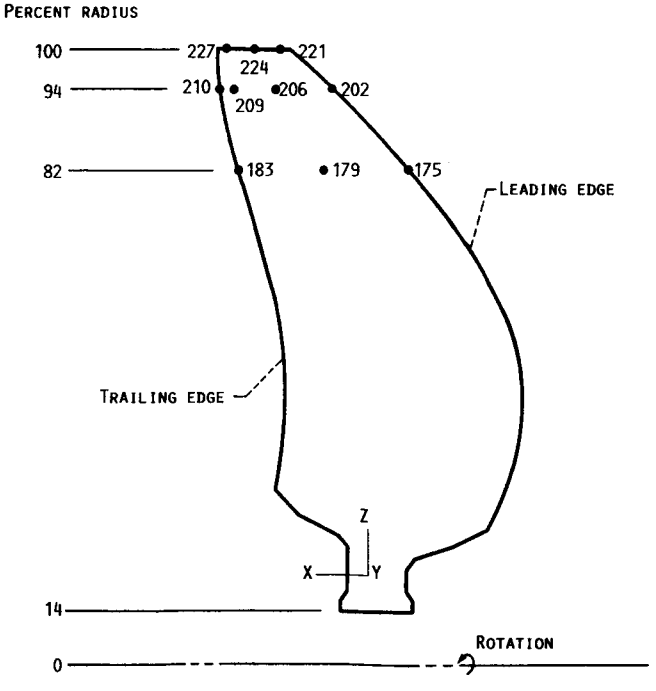

FIGURE 2.- MASS LOCATIONS ON SR3C-X2 BLADE.

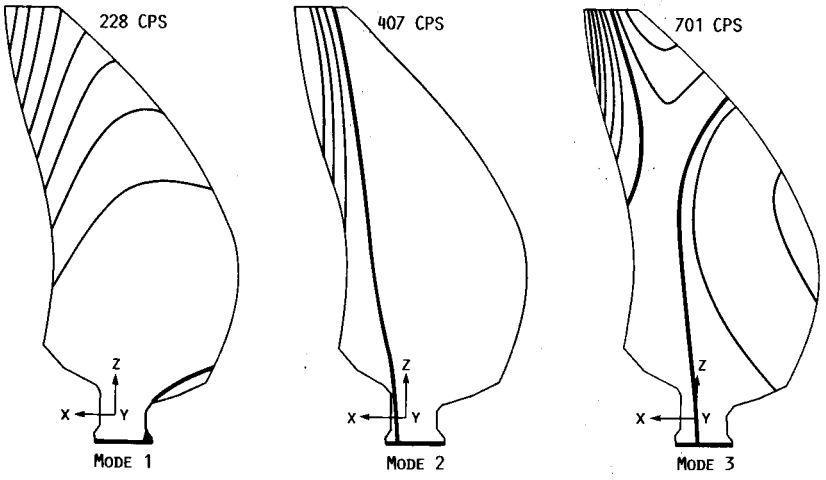

FIGURE 3.- NATURAL MODE CONTOURS OF CONSTANT Y DISPLACEMENT AND FREQUENCIES OF THE SR3C-X2 WITH NO CONCENTRATED MASS (6950 RPM, BLADE SETTING ANGLE 56.4 DEG).

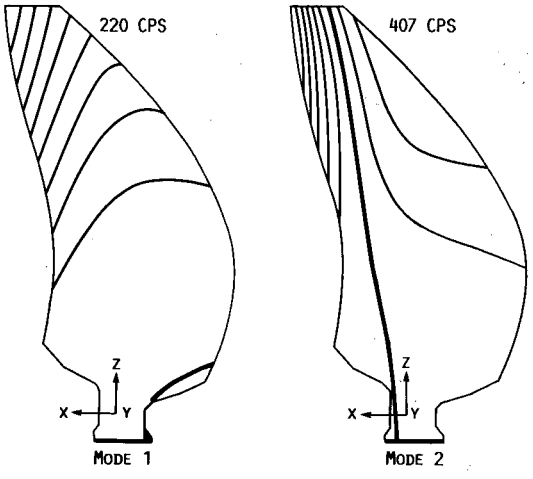

FIGURE 4.- NATURAL MODE CONTOURS OF CONSTANT Y DISPLACEMENT AND FREQUENCIES WHEN 0.5% MASS IS LOCATED AT 13% CHORD AT THE 100% RADIUS (6950 RPM, BLADE SETTING ANGLE 56.4 DEG).

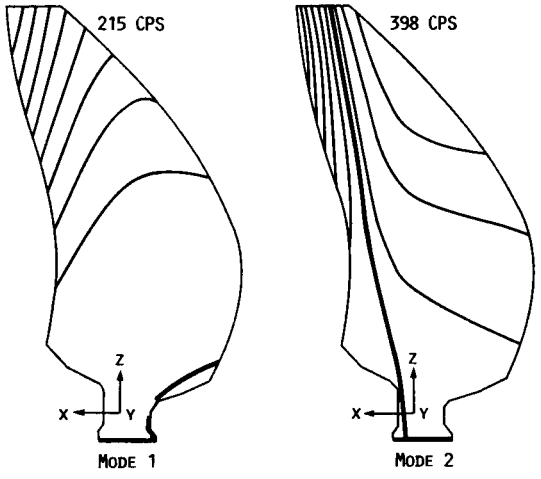

FIGURE 5.- NATURAL MODE CONTOURS OF CONSTANT Y DISPLACEMENT AND FREQUENCIES WHEN 0.5% MASS IS LOCATED AT 51% CHORD AT THE 100% RADIUS (6950 RPM, BLADE SETTING ANGLE 56.4 DEG).

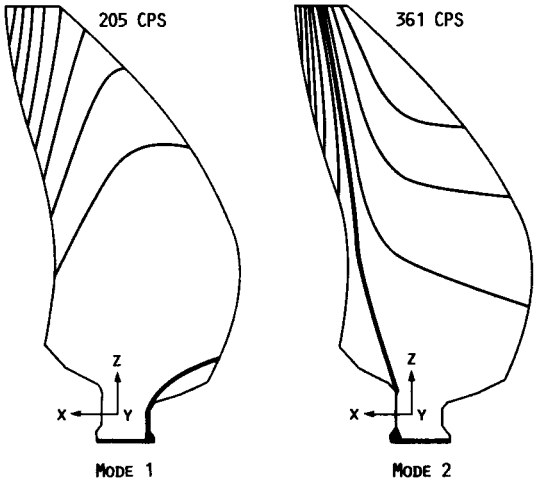

FIGURE 6.- NATURAL MODE CONTOURS OF CONSTANT Y DISPLACEMENT AND FREQUENCIES WHEN 0.5% MASS IS LOCATED AT 88% CHORD AT THE 100% RADIUS (6950 RPM, BLADE SETTING ANGLE 56.4 DEG).

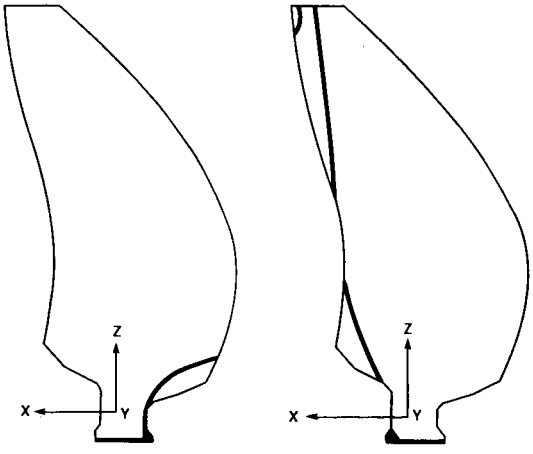

MODE 1 MODE 2

FIGURE 7.- NODAL LINES OF THE FIRST AND SECOND MODES WHEN THE 1.0% MASS WAS LOCATED AT 100% CHORD AT THE 94% RADIUS (6950 RPM, BLADE SETTING ANGLE 56.4 DEG).

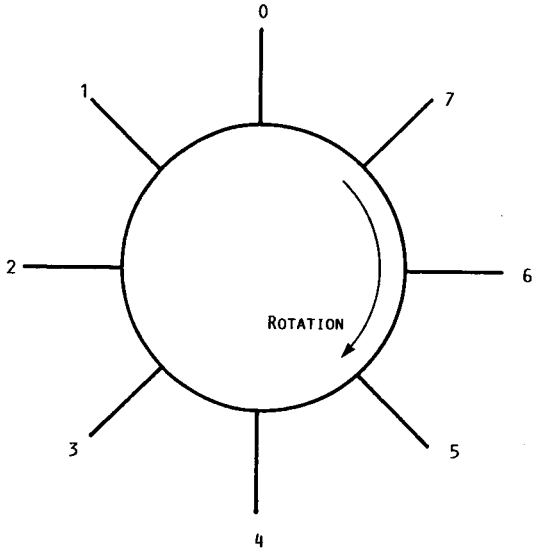

FIGURE 8.- BLADE NUMBERING CONVENTION.

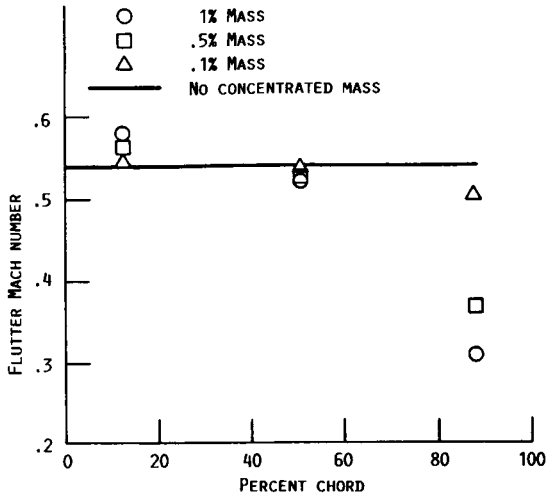

FIGURE 9.- FLUTTER MACH NUMBER VERSUS PERCENT CHORD, 100 PERCENT RADIUS, RPM = 6950.

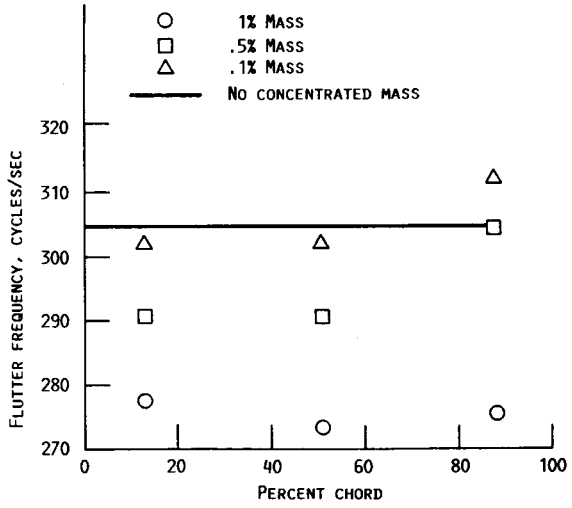

FIGURE 10.- FLUTTER FREQUENCY VERSUS PERCENT CHORD, 100 PERCENT RADIUS, RPM = 6950.

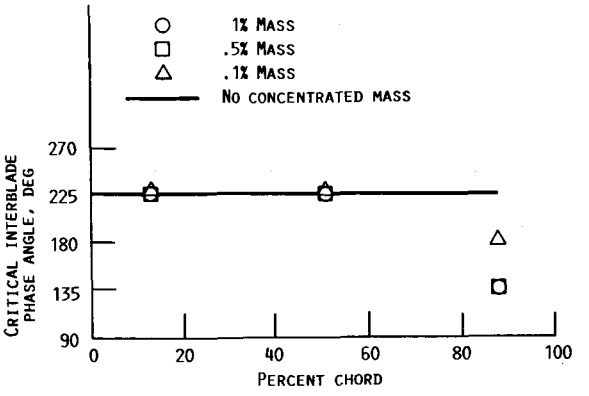

FIGURE 11.- CRITICAL INTERBLADE PHASE ANGLE VERSUS PERCENT CHORD, 100 PERCENT RADIUS, RPM = 6950.

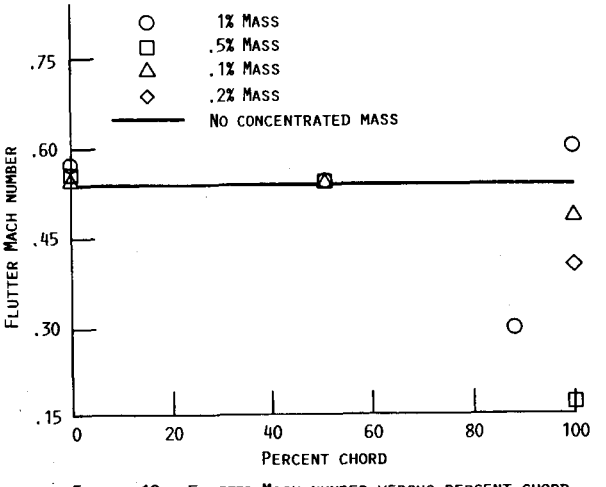

FIGURE 12.- FLUTTER MACH NUMBER VERSUS PERCENT CHORD, 94 PERCENT RADIUS, RPM = 6950.

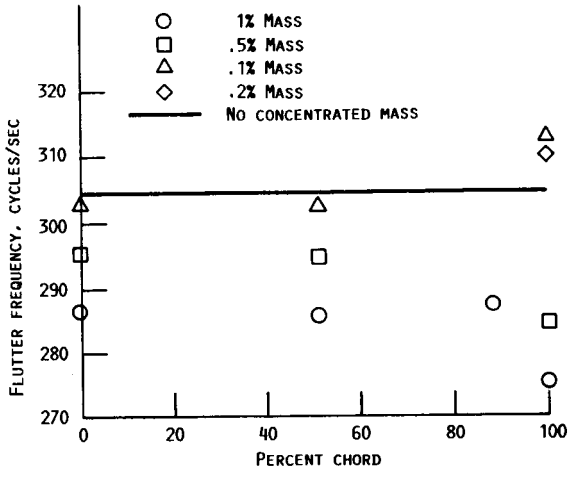

FIGURE 13.- FLUTTER FREQUENCY VERSUS PERCENT CHORD, 94 PERCENT RADIUS, RPM = 6950.

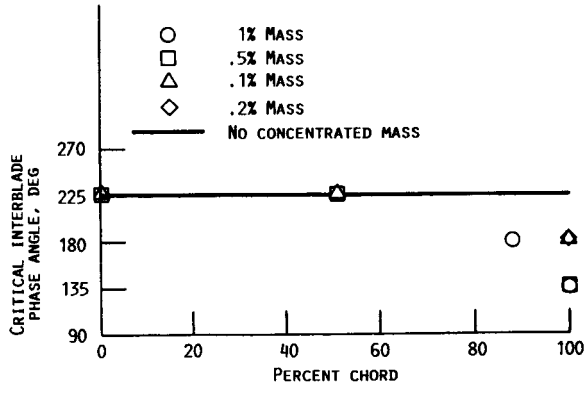

FIGURE 14.- CRITICAL INTERBLADE PHASE ANGLE VERSUS PERCENT CHORD, 94 PERCENT RADIUS, RPM = 6950.

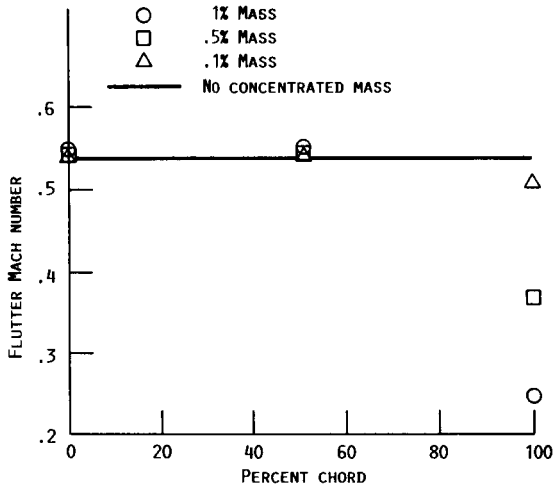

FIGURE 15.- FLUTTER MACH NUMBER VERSUS PERCENT CHORD, 82 PERCENT RADIUS, RPM = 6950.

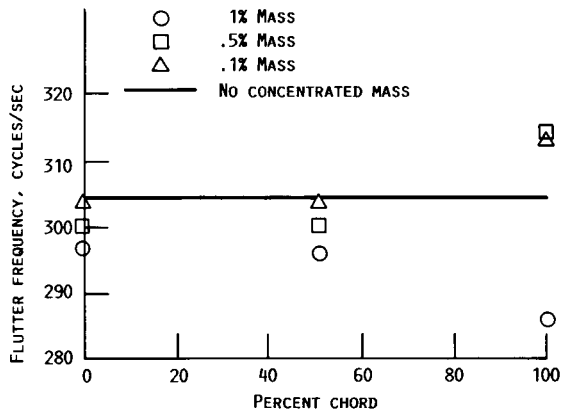

FIGURE 16.- FLUTTER FREQUENCY VERSUS PERCENT CHORD, 82 PERCENT RADIUS, RPM = 6950.

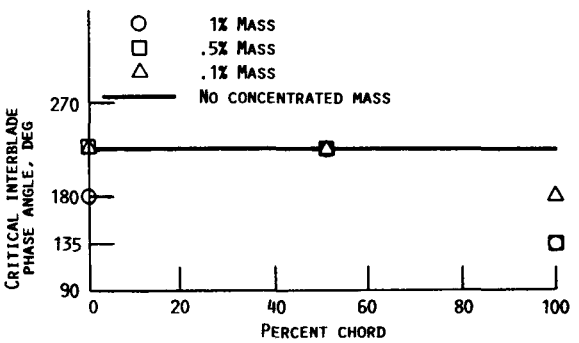

FIGURE 17.- CRITICAL INTERBLADE PHASE ANGLE VERSUS PERCENT CHORD, 82 PERCENT RADIUS, RPM = 6950.

1. Report No.	2. Government Accession No.	3. Recipient's Catalog No.
NASA TM-88854		

4. Title and Subtitle	5. Report Date
Concentrated Mass Effects on the Flutter of a Composite Advanced Turboprop Model	October 1986
	6. Performing Organization Code: 535-03-01
7. Author(s): J.K. Ramsey and K.R.V. Kaza	8. Performing Organization Report No.: E-3247
	10. Work Unit No.
9. Performing Organization Name and Address: National Aeronautics and Space Administration, Lewis Research Center, Cleveland, Ohio 44135	11. Contract or Grant No.
	13. Type of Report and Period Covered: Technical Memorandum
12. Sponsoring Agency Name and Address: National Aeronautics and Space Administration, Washington, D.C. 20546	14. Sponsoring Agency Code

15. Supplementary Notes

16. Abstract

The effects on bending-torsion flutter due to the addition of a concentrated mass to an advanced turboprop model blade with rigid hub are studied. Specifically the effects of the magnitude and location of added mass on the natural frequencies, mode shapes, critical interblade phase angle, and flutter Mach number are analytically investigated. The flutter of a propfan model is shown to be sensitive to the change in mass distribution. Static unbalance effects, like those for fixed wings, were shown to occur as the concentrated mass was moved from the leading edge to the trailing edge with the exception of one mass location. Mass balancing is also inferred to be a feasible method for increasing the flutter speed.

17. Key Words (Suggested by Author(s))	18. Distribution Statement
Flutter; Propfans; Turboprop; Mass balancing	Unclassified - unlimited STAR Category 39

19. Security Classif. (of this report)	20. Security Classif. (of this page)	21. No. of pages	22. Price*
Unclassified	Unclassified		

*For sale by the National Technical Information Service, Springfield, Virginia 22161